A generalized cortical activity pattern at internally-generated mental context boundaries during unguided narrative recall

Hongmi Lee[1*], Janice Chen[1]

[1]Department of Psychological and Brain Sciences,
Johns Hopkins University,
Baltimore, MD 21218, USA

*Correspondence: Hongmi Lee (hongmi.lee@jhu.edu)

Abstract

Current theory and empirical studies suggest that humans segment continuous experiences into events based on the mismatch between predicted and actual sensory inputs; detection of these "event boundaries" evokes transient neural responses. However, boundaries can also occur at transitions between internal mental states, without relevant external input changes. To what extent do such "internal boundaries" share neural response properties with externally-driven boundaries? We conducted an fMRI experiment where subjects watched a series of short movies and then verbally recalled the movies, unprompted, in the order of their choosing. During recall, transitions between movies thus constituted major boundaries between internal mental contexts, generated purely by subjects' unguided thoughts. Following the offset of each recalled movie, we observed stereotyped spatial activation patterns in the default mode network, especially the posterior medial cortex, consistent across different movie contents and even across the different tasks of movie watching and recall. Surprisingly, the between-movie boundary patterns were negatively correlated with patterns at boundaries between events within a movie. Thus, major transitions between mental contexts elicit neural phenomena shared across internal and external modes and distinct from within-context event boundary detection, potentially reflecting a cognitive state related to the flushing and reconfiguration of situation models.

Introduction

Humans perceive and remember continuous experiences as discrete events (Brunec et al., 2018; Clewett et al., 2019; Shin & DuBrow, 2021; Zacks, 2020). Studies of event segmentation have shown that when participants attend to external information (e.g., watch a video), 1) boundaries between events are detected when mismatches arise between predicted and actual sensory input (Zacks et al., 2007, 2011), and 2) boundary detection evokes transient neural responses in a consistent set of brain areas (Speer et al., 2007; Zacks et al., 2001; Zheng et al., 2021). Among these areas is the default mode network (DMN; Buckner & DiNicola, 2019) proposed to be involved in representing complex mental models of events (Ranganath & Ritchey, 2012; Ritchey & Cooper, 2020). However, a substantial portion of human cognition is internally-driven (Hasselmo, 1995; Honey et al., 2017), and such spontaneous production of thoughts and actions is also punctuated by mental context transitions (Christoff et al., 2016; Mildner & Tamir, 2019; Smallwood & Schooler, 2015; Tseng & Poppenk, 2020). What manner of brain activity marks boundaries between mental contexts when they are internally-generated? Are the brain responses at internal boundaries similar to those at external boundaries?

Here, we used naturalistic movie viewing and free spoken recall with fMRI to characterize neural activity at boundaries between internally-generated mental contexts (Figure 1A). Subjects watched ten short movies (encoding phase), then verbally recounted the movies in any order, in their own words (recall phase). The transitions between recalled movies were determined purely by subjects' internal mentation; no external cues prompted the recall onset or offset of each movie. Moreover, the unguided spoken recall allowed us to identify the exact moments of context transitions and explicitly track shifts in the contents of thoughts (Chen et al., 2017; Sripada & Taxali, 2020), which was not possible in prior studies using silent rest (Karapanagiotidis et al., 2020; Tseng & Poppenk, 2020). We observed limited changes in univariate activity at these internal boundaries between recalled movies. However, we observed transient, highly generalizable and fine-grained activation patterns throughout the DMN, consistent across diverse movie contents and similar to those at external between-movie boundaries during encoding. Moreover, these between-movie boundary patterns were not merely stronger versions of within-movie "event boundaries", but instead manifested as a distinct type of neural transition. We propose that these cortical patterns reflect a cognitive state related to the flushing and reconfiguration of mental context (DuBrow et al., 2017; Manning et al., 2016).

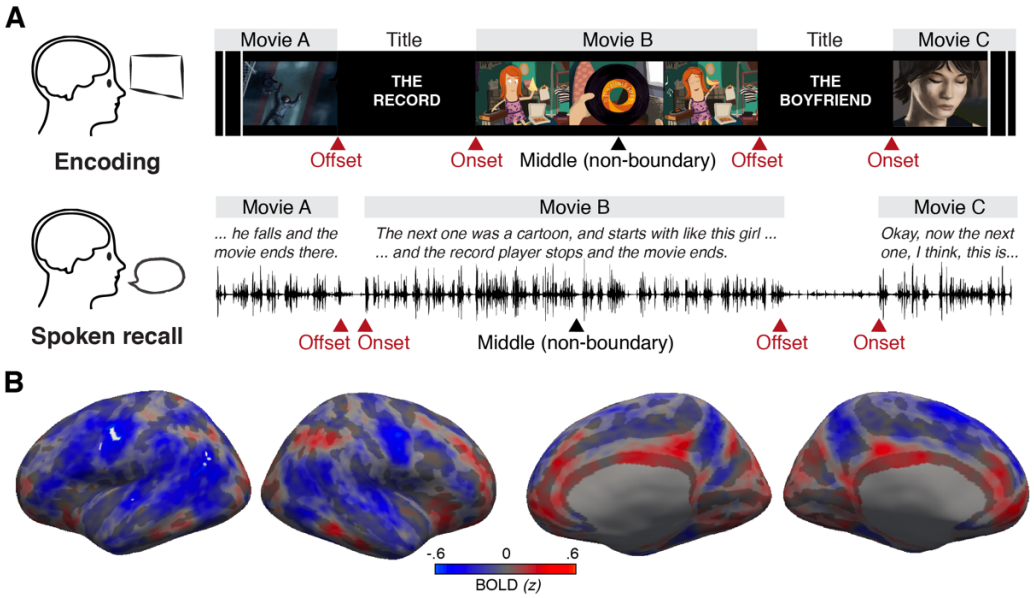

Figure 1. Experimental procedures and univariate responses. (A) In the encoding phase, subjects watched 10 short movies approximately 2 to 8 minutes long. Each movie started with a 6-second title scene. In the free spoken recall phase, subjects verbally recounted each movie plot in as much detail as possible regardless of the order of presentation. After recalling one movie, subjects spontaneously proceeded to the next movie, and the transitions between movies were considered as internally-driven boundaries. Red arrows indicate the boundaries (onsets and offsets) between watched or recalled movies. Black arrows indicate the non-boundary moments (middle) of each watched or recalled movie. (B) Whole-brain maps of mean activation (BOLD signals z-scored across all volumes within a scanning run) following between-movie boundaries during recall (4.5 – 19.5 seconds from the offset of each movie). Blue areas indicate regions with lower-than-average activation. Red areas indicate regions with higher-than-average activation. White dots on the lateral surface of the left hemisphere (the leftmost map) indicate vertices that showed significantly lower activation following between-movie boundaries compared to non-boundary periods (Bonferroni corrected $p < .05$). The non-boundary periods were defined as the middle 15 seconds of each recalled movie, shifted forward by 4.5 seconds. Changes in whole-brain univariate responses across time around the boundaries are shown in Figure 1 supplement video 1 (recall phase) and Figure 1 supplement video 2 (encoding phase).

Results and discussion

We first examined whether internally-driven boundaries evoke changes in blood oxygen level-dependent (BOLD) signals during recall. We observed limited transient changes in activation at the boundaries between recalled movies in multiple cortical regions; a whole-brain analysis with multiple comparisons correction revealed that the mean activation of boundary periods (15 seconds following the offset of each movie) was lower than that of non-boundary periods (middle 15 seconds within each movie) in a small number of vertices within the left motor, auditory, and inferior parietal cortices (Figure 1B), although weaker responses were observed in widespread cortical regions (Figure 1 supplement video 1).

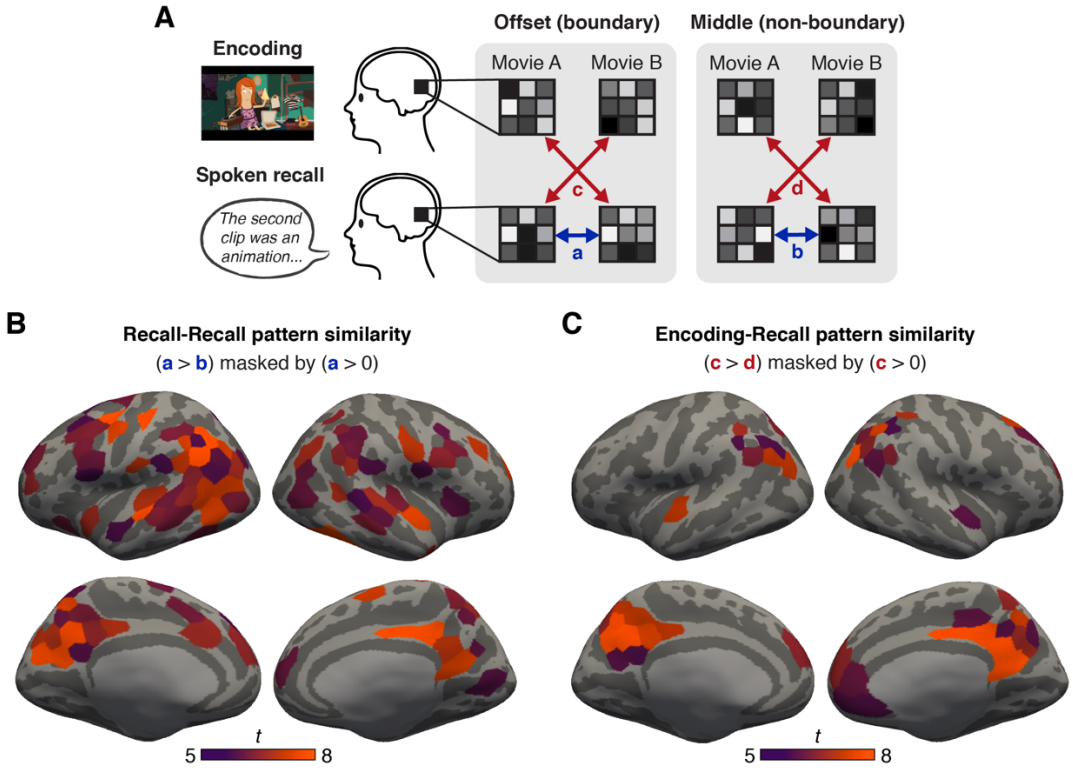

Figure 2. Consistent activation patterns associated with between-movie boundaries. (A) Schematic of the pattern similarity analysis. Boundary patterns were defined as the mean pattern averaged across 15 seconds following the offset of each watched or recalled movie. Non-boundary patterns were defined as the mean pattern averaged across 15 seconds in the middle of each watched or recalled movie. For each subject and cortical parcel (Schaefer et al., 2018; 200 parcels per hemisphere), we computed pairwise between-movie pattern similarity (Pearson correlation), separately for boundary patterns and non-boundary patterns measured during recall (a & b, blue arrows). We also computed between-movie and between-phase (encoding-recall) pattern similarity, again separately for boundary and non-boundary patterns (c & d, red arrows). The time windows for both boundary and non-boundary periods were shifted forward by 4.5 seconds to account for the hemodynamic response delay. (B) Whole-brain *t* statistic map of cortical parcels that showed consistent between-movie boundary patterns during recall. These parcels displayed significantly greater between-movie pattern similarity in the boundary condition compared to the non-boundary condition during recall. The map was masked by parcels that showed significantly positive between-movie pattern similarity in the boundary condition during recall. Both effects were Bonferroni corrected across parcels ($p < .05$). (C) Whole-brain *t* statistic map of cortical parcels that showed consistent between-movie boundary patterns across encoding and recall. These parcels displayed significantly greater between-movie and between-phase pattern similarity in the boundary condition compared to the non-boundary condition. The map was masked by parcels that showed significantly positive between-movie and between-phase pattern similarity in the boundary condition. Both effects were Bonferroni corrected across parcels ($p < .05$).

Next, we tested whether there were neural activation *patterns* specific to internally-driven boundaries and consistent across different movies. We performed a whole-brain pattern similarity analysis on the recall data to identify regions where 1) boundary period activation patterns were positively correlated across different recalled movies, and 2) this correlation was

higher at boundaries than at non-boundaries (Figure 2A, blue arrows). We observed a consistent boundary pattern, i.e., whenever participants transitioned from talking about one movie to the next, in several cortical parcels (Schaefer et al., 2018) including the DMN and auditory/motor areas (Figure 2B), suggesting the involvement of both cognitive and sensory/motor factors at recall boundaries (e.g., breaks in recall speech generation and memory retrieval).

To what extent is the internally-driven boundary pattern, measured during recall, similar to patterns observed at boundaries during encoding? To test this, we again computed between-movie pattern similarity, but now across the encoding and recall phases (Figure 2A, red arrows). We found that DMN areas, especially the posterior medial cortex (PMC), showed a consistent boundary pattern across task phases (encoding and recall) and across movies (Figure 2C). Thus, we next examined the phenomenon in more detail specifically in PMC. Figures 3A and 3C visualize the high and consistently positive correlations of PMC boundary patterns across different movies both within the recall phase (Recall Offset vs. Recall Offset, $t(14) = 11.82$, $p < .001$, Cohen's $d_z = 3.05$) and even between experimental phases (Recall Offset vs. Encoding Offset, $t(14) = 14.54$, $p < .001$, Cohen's $d_z = 3.75$). No such correlation was present between non-boundary patterns ($t(14)$s < 1, ps $> .3$). Individual subjects' activation maps visualize the similarity between boundary patterns during encoding and recall (Figure 3B, Figure 3 supplement 1). We observed similar results in the lateral parietal DMN sub-region (angular gyrus; Figure 3 supplement 2). This observation of a generalized boundary pattern in DMN regions extends prior reports of DMN univariate responses at external event boundaries (Reagh et al., 2020; Speer et al., 2007) and transitions between tasks (Crittenden et al., 2015; Smith et al., 2018).

Is the generalized boundary pattern evoked by the offset or onset of a movie? Thus far, we tested boundary responses following offsets, based on prior findings that post-stimulus neural responses contribute to memory formation (Ben-Yakov et al., 2013; Ben-Yakov & Dudai, 2011; Medvedeva et al., 2021). However, other studies reported neural responses specific to the onset of an episode (Bulkin et al., 2020; Fox et al., 2005; Wen et al., 2020). We computed between-phase (encoding-recall) pattern similarity across individual time points, time-locked to either the onset or offset of each watched or recalled movie (Figure 3D). We found that significantly positive between-phase correlations emerged before the encoding and recall onsets, starting from 4.5 seconds following the offsets of the preceding movie. Thus, it is likely that boundary patterns were driven primarily by offset responses.

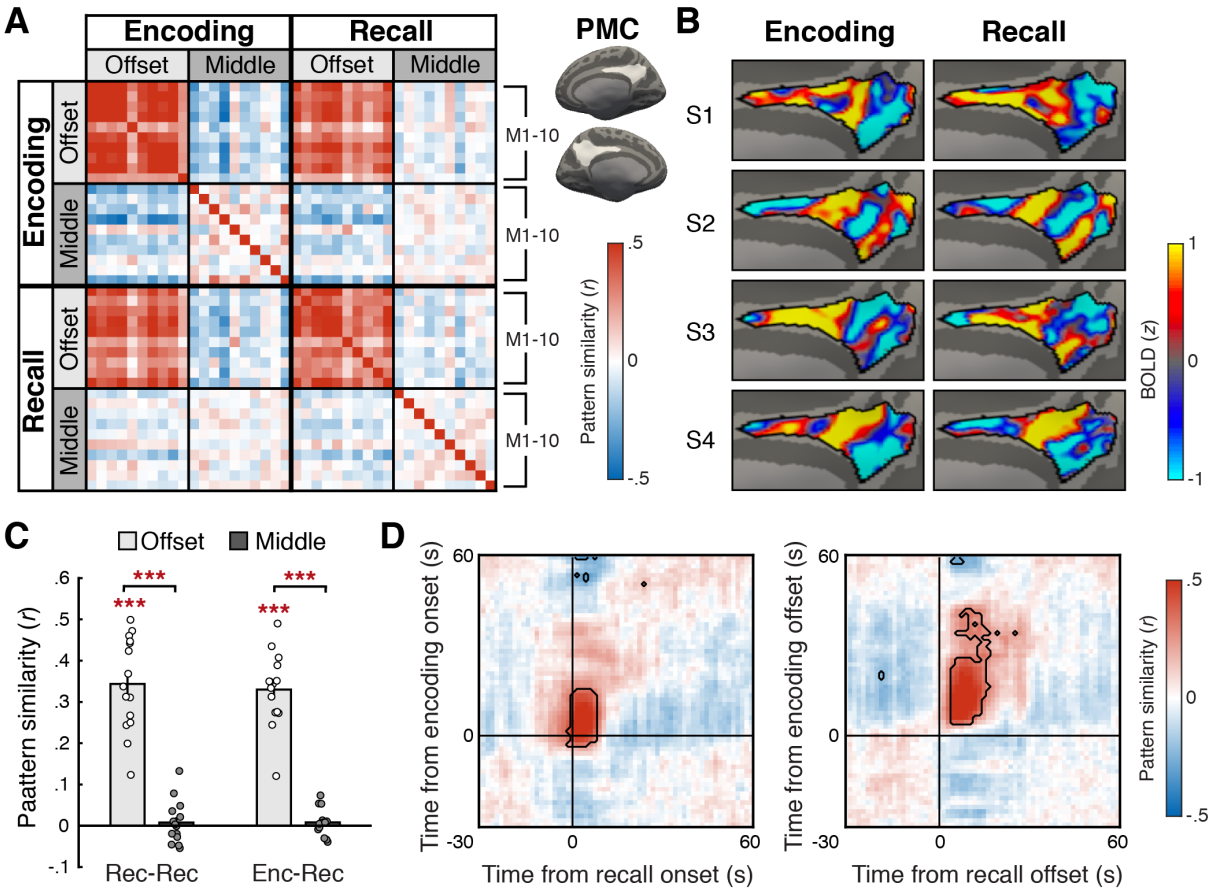

Figure 3. Boundary pattern in the posterior medial cortex (PMC). (A) PMC activation pattern similarity (Pearson correlation) between the 10 movie stimuli (M1 – 10), conditions (Offset = boundary, Middle = non-boundary), and experimental phases (Encoding, Recall), averaged across all subjects. The boundary pattern of a movie was defined as the mean pattern averaged across the 15-second window following the offset of the movie. The non-boundary pattern was defined as the mean pattern averaged across the 15-second window in the middle of a movie. The time windows for both boundary and non-boundary patterns were shifted forward by 4.5 seconds to account for the hemodynamic response delay. PMC regions of interest are shown as white areas on the inflated surface of a template brain. (B) Subject-specific mean activation patterns associated with between-movie boundaries during encoding (left) and recall (right). The boundary patterns were averaged across all movies and then *z*-scored across vertices within the PMC ROI mask, separately for each experimental phase. PMC (demarcated by black outlines) of four example subjects (S1 – 4) are shown on the medial surface of the right hemisphere of the fsaverage6 template brain. (C) Within-phase (Recall-Recall) and between-phase (Encoding-Recall) pattern similarity across different movies, computed separately for the boundary (Offset) and non-boundary (Middle) patterns in PMC. Bar graphs show the mean across subjects. Circles represent individual subjects. Error bars show SEM across subjects. ***$p < .001$. (D) Time-point-by-time-point PMC pattern similarity across the encoding phase and recall phase activation patterns around between-movie boundaries, averaged across all subjects. The time series of activation patterns were locked to either the onset (left) or the offset (right) of each movie. During encoding, the onset of a movie and the offset of the preceding movie were separated by a 6-second title scene. During recall, onsets and offsets of recalled movies were separated by, on average, a 9.3-second pause (boundaries concatenated across subjects, SD = 16.8 seconds). Note that in this figure, zero corresponds to the true stimulus/behavior time, with no shifting for hemodynamic response delay. Areas outlined by black lines indicate correlations significantly different from zero after multiple comparisons correction (Bonferroni corrected $p < .05$). Time-time correlations within each experimental phase can be found in Figure 3 supplement 3.

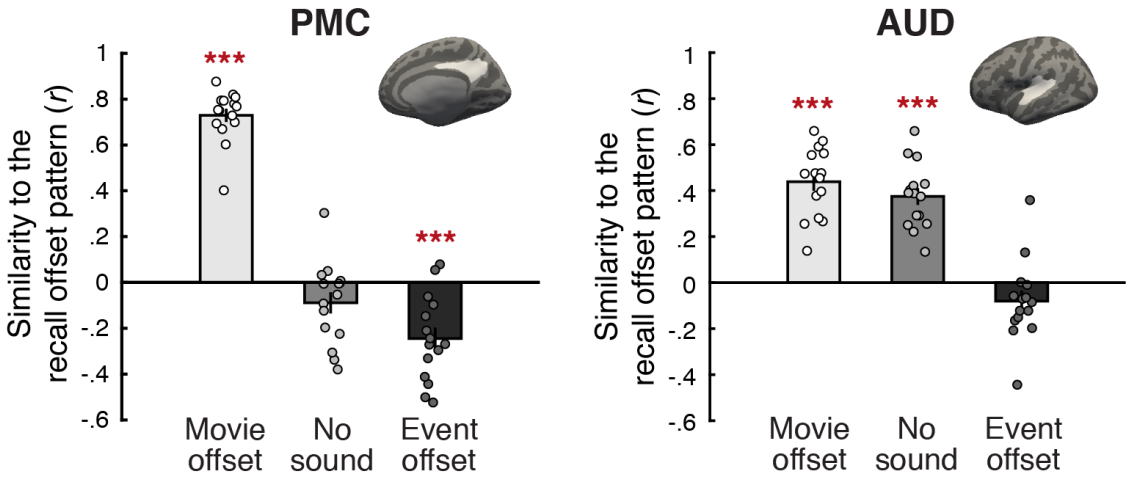

Figure 4. Comparisons between template patterns. We measured the similarity (Pearson correlation) between the average between-movie boundary pattern during recall and average encoding patterns associated with 1) between-movie boundaries (Movie offset), 2) silence (No sound), and 3) major within-movie event boundaries (Event offset) in the posterior medial cortex (PMC; left panel) and the auditory cortex (AUD; right panel). The regions of interest are shown as white areas on the inflated surface of a template brain. Bar graphs show the mean across subjects. Circles represent individual subjects. Error bars show SEM across subjects. ***p < .001 against zero.

We focused our analyses up to this point on transitions between movies because they provided clear boundaries between mental contexts during recall. Yet, event boundaries in naturalistic movie stimuli are often defined as transitions between scenes within a movie (Baldassano et al., 2017; Chen et al., 2017; Zacks et al., 2010). In prior work, it has been shown that for within-movie event boundaries, neural responses scale positively with human judgments of the ”strength” of scene transitions (Ben-Yakov & Henson, 2018). Thus, we hypothesized that boundaries between movies (i.e., between mental contexts) would manifest as stronger versions of within-movie boundaries. We correlated 1) the mean between-movie boundary pattern during recall and 2) the mean within-movie event boundary pattern during encoding, in PMC (Figure 4, ‘Event offset’ condition). Surprisingly, the two were negatively correlated ($t(14)$ = 5.10, p < .001, Cohen’s d_z = 1.32), suggesting that the between-movie boundary pattern may reflect a cognitive state qualitatively different from the state elicited by event boundaries during movie watching (e.g., attentional engagement; Song et al., 2021).

Is the generalized boundary pattern driven by shared low-level perceptual or motoric factors rather than cognitive states? Visual features (i.e., black screen) or pauses in speech cannot explain boundary-specific similarity between encoding and recall phases, because boundary and non-boundary periods were identical in terms of visual input during recall and

speech generation during movie watching. Moreover, PMC boundary patterns showed positive between-phase pattern correlations ($t(14) = 3.94$, $p = .003$, Cohen's $d_z = 1.25$) greater than those of non-boundary patterns ($t(14) = 3.22$, $p = .011$, Cohen's $d_z = 1.02$) even when restricted to boundaries without pauses between recalled movies. We also ruled out the possibility that silence during movie title scenes and pauses at recall boundaries drove the generalized boundary pattern in PMC; the recall boundary pattern was not correlated with the pattern associated with silent periods during encoding ($t(14) = 1.93$, $p = .074$, Cohen's $d_z = .498$), whereas the auditory cortex showed a positive correlation between the two ($t(14) = 10.31$, $p < .001$, Cohen's $d_z = 2.66$) (Figure 4, 'No sound' condition). Likewise, the movies' audio amplitudes modulated the time course of similarity between the recall boundary pattern and the encoding data in the auditory cortex, but not in PMC (Figure 4 supplements 1, 2).

Our study demonstrates that internally-generated boundaries between mental contexts during narrated memory recall evoke generalized neural activation patterns in core posterior-medial areas of the DMN (Ritchey & Cooper, 2020). These cortical patterns were similar to those observed at major transitions between externally-driven contexts (different audiovisual movies), suggesting that they reflect a general cognitive state associated with mental context transitions. Importantly, these between-context patterns were distinct from within-context event boundary detection signals. We speculate that the boundary state may be a temporary "relay" state that occurs when no one mental model wins the competition to receive full attentional focus (e.g., attention lapse, off-focus, mind-blanking; deBettencourt et al., 2018; Mittner et al., 2016; Mortaheb et al., 2021; Ward & Wegner, 2013) following the flushing of the prior mental context. An alternative, but not mutually exclusive, possibility is that the boundary state involves the recruitment of cognitive control to resolve the competition between mental contexts; the relative activation of the frontoparietal control network interdigitated with the DMN (Braga & Buckner, 2017) may contribute to the generalized boundary pattern.

The current study focused on the boundaries between narratives involving multiple entities and their interactions, and thus the transition may coincide with the reconfiguration of situation models represented in the DMN (Ranganath & Ritchey, 2012). Future studies may investigate whether the boundary pattern we observed is associated specifically with detachment from situation-level information accumulated over long timescales (Hasson et al., 2015), or also with detachment from relatively simple and brief stimulus or task contexts (e.g., Crittenden et al., 2015; Kragel & Polyn, 2015; Schapiro et al., 2013). Our results also lay the groundwork for future studies to examine the possible utility of these "relay" states in comprehension, learning, and building durable memories.

Materials and methods

Here, we provide a selective overview of procedures and analysis methods. More detailed descriptions of participants, stimuli, experimental procedures, fMRI data acquisition and preprocessing can be found in Lee & Chen (2021).

Participants

Twenty-one subjects (12 females) between the ages of 20 and 33 participated in the study. Informed consent was obtained in accordance with procedures approved by the Princeton University Institutional Review Board. Six subjects were excluded from analyses due to excessive motion.

Stimuli

Ten audiovisual movies (ranged 2.15 – 7.75 minutes) were used in the experiment. The movies varied in format (animation, live-action) and content. Each movie clip was prepended with a title scene where the movie title in white letters faded in and out at the center of the black screen. The movie title was shown approximately for 3 seconds of the 6-second long title scene. At the beginning of each scanning run, a 39-second long audiovisual introductory cartoon was played before the movie stimuli. The introductory cartoon was excluded from analyses.

Experimental procedures

The experiment consisted of two phases, encoding and free spoken recall (Figure 1A), both performed inside the MRI scanner. In the encoding phase, subjects watched a series of ten short movies. Subjects were instructed to pay attention to the movies, and no behavioral responses were required. There were two scanning runs, and subjects watched five movies in each run. Stimulus presentation began 3 seconds after the first volume of each run. In the free spoken recall phase, subjects were instructed to verbally recount what they remembered from the movies, regardless of the order of presentation. Subjects were encouraged to describe their memory in their own words in as much detail as possible. A white dot was presented in the center of the black screen during the free spoken recall phase, though subjects were not required to fixate. Subjects' recall speech was audio-recorded using an MR-compatible noise-cancelling microphone and then manually transcribed. The recall transcripts were also timestamped to identify the onset and offset of the description of each movie (there were no

intrusions across movies during recall).

fMRI acquisition and preprocessing

Imaging data were collected on a 3T Siemens Prisma scanner at Princeton Neuroscience Institute. Functional images were acquired using a T2*- weighted multiband accelerated echo-planar imaging sequence (TR = 1.5 s; TE = 39 ms; flip angle = 50°; acceleration factor = 4; 60 slices; 2 × 2 × 2 mm^3). Whole-brain anatomical images and fieldmap images were also acquired. Functional images were motion-corrected and unwarped using FSL, and then coregistered to the anatomical image, resampled to the fsaverage6 cortical surface, and smoothed (FWHM 4 mm) using FreeSurfer Functional Analysis Stream. The smoothed data were also high-pass filtered (cutoff = 140 s) and z-scored within each scanning run. The first 5 volumes of encoding scanning runs and the first 3 volumes of free spoken recall scanning runs were excluded from analyses.

Cortical parcellation and region of interest (ROI) definition

For whole-brain pattern similarity analysis, we used an atlas (Schaefer et al., 2018) which divided the cortical surface into 400 parcels (200 parcels per hemisphere) based on functional connectivity patterns (17 networks version). For region-of-interest analyses, we defined the bilateral posterior-medial cortex (PMC) by combining the parcels corresponding to the precuneus and posterior cingulate cortex within Default Network A. The bilateral auditory cortex ROI was defined by combining the parcels corresponding to the primary and secondary auditory cortices within Somatomotor Network B. The bilateral angular gyrus ROI consisted of the parcels corresponding to the inferior parietal cortex within Default Network A, B and C.

Univariate activation analysis

We performed whole-brain univariate activation analysis to identify brain areas that show activation changes at between-movie boundaries compared to non-boundary periods during recall (Figure 1B). The boundary periods were the first 15 seconds following the offset of each recalled movie, and the non-boundary periods were the 15 seconds in the middle of each recalled movie. Both boundary and non-boundary period time windows were shifted forward by 4.5 seconds to account for the hemodynamic response delay. For each vertex in each subject's brain, we computed the mean boundary activation by first averaging preprocessed BOLD signals across time points within each boundary period, and then across all recalled movies. Likewise, we computed the mean non-boundary activation for each subject and vertex by first

averaging preprocessed BOLD signals across time points within each non-boundary period, and then across all recalled movies. We then computed the difference between the boundary and non-boundary activation for each subject. Finally, we performed a group-level one-sample *t*-test against zero (two-tailed). Bonferroni correction was applied to correct for multiple comparisons across vertices on the resulting whole-brain statistical parametric map.

Pattern similarity analysis

We performed whole-brain pattern similarity analysis (Figure 2A) to identify brain areas that showed content-and task-general neural activation patterns associated with between-movie boundaries. For each cortical parcel of each subject's brain, we extracted boundary and non-boundary activation patterns for each movie, separately for the encoding phase and the recall phase. Boundary patterns were generated by averaging the spatial patterns of activation within the boundary period (the first 15 seconds following the offset) of each watched or recalled movie. Non-boundary patterns were generated by averaging spatial patterns within the non-boundary period (the middle 15 seconds) of each watched or recalled movie. Again, both boundary and non-boundary time windows were shifted forward by 4.5 seconds to account for the hemodynamic response delay. We then computed Pearson correlation coefficients between the patterns within and across different movies, conditions (boundary, non-boundary), and experimental phases.

Using the resulting correlation matrix (see Figure 3A for an example) for each parcel, we first identified brain areas that showed boundary patterns which were consistent *across recalled movies* (Figure 2B). For each subject's recall phase, we computed the mean of all pairwise between-movie correlations, separately for the boundary patterns and the non-boundary patterns. We then performed a group-level two-tailed one-sample *t*-test against zero on the mean boundary pattern correlations to test whether the boundary pattern similarity was overall positive. We also performed a group-level two-tailed paired-samples *t*-test between the mean boundary vs. non-boundary pattern correlations to test whether the boundary pattern similarity was greater than the non-boundary pattern similarity. Each of the resulting whole-brain statistical parametric maps was corrected for multiple comparisons across parcels using the Bonferroni method. Finally, we identified parcels that showed significant effects in both tests after the correction (Figure 2B). Likewise, we identified brain areas that showed boundary patterns which were consistent *across the encoding and recall phases* as well as across movies (Figure 2C). This was achieved by repeating the identical analysis procedures using the boundary and non-boundary pattern correlations computed across the encoding and recall

phases, instead of using the correlations computed within the recall phase.

We also performed the same pattern similarity analysis in the PMC (Figure 3) and angular gyrus (Figure 3 supplement 2) ROIs, as done for an individual cortical parcel in the whole-brain analysis.

Comparing the onset- and offset-locked boundary patterns

To test whether the consistent activation patterns associated with between-movie boundaries were evoked by the onset or offset of a movie, we examined TR-by-TR pattern correlations across time points around the boundaries. The time points were locked to either the onset or the offset of 1) each video clip (excluding the title scene) or 2) recall of each movie. For each subject and ROI, we extracted the time series of activation patterns from 30 seconds before to 60 seconds after the onset/offset of each watched or recalled movie. We averaged the time series across movies to create a single time series of boundary-related activation patterns per experimental phase. We then computed Pearson correlation coefficients across different time points in the time series of mean activation patterns within each experimental phase (i.e., encoding-encoding and recall-recall correlation; Figure 3 supplement 3) or between phases (i.e., encoding-recall correlation; Figure 3D, Figure 3 supplement 2D). Finally, we performed two-tailed one-sample *t*-tests against zero on each cell of the time-time correlation matrices from all subjects to identify the time points at which positive pattern correlations appeared. Bonferroni correction was applied to correct for multiple comparisons across all cells in the time-time correlation matrix.

Comparing the between-movie and within-movie boundary patterns

To test whether the recall activation patterns evoked by between-movie boundaries were similar to encoding activation patterns evoked by event boundaries within a movie (Figure 4, 'Event offset' condition), we identified the strongest event boundaries within each movie. We utilized the fine-grained event boundaries defined in our previous study (Lee & Chen, 2021) which divided the ten movie stimuli into 202 events excluding title scenes (mean duration = 13.5 seconds, ranged 2 – 42 seconds). We had four independent coders watch the movie stimuli and then choose which of the fine-grained event boundaries were the most important. The coders were instructed to select the boundaries such that the ten movies were divided into 60 ± 10 events excluding title scenes. Of these, 25 event boundaries were identified as important by all four coders, which resulted in 27 "coarse" events in total (ranging between one and five events per movie; mean duration = 100.9 seconds, ranged 21 – 417 seconds). To mitigate the

possibility of carryover effects from the between-movie boundaries, within-movie event boundaries that occurred within the first 45 seconds of each movie clip were excluded from the analysis, leaving 15 within-movie event boundaries in total. For each subject, we generated the mean within-movie event boundary pattern of an ROI by averaging activation patterns from 4.5 to 19.5 seconds following each of the 15 event boundaries during encoding. Likewise, the mean between-movie boundary pattern was generated by averaging all activation patterns from 4.5 to 19.5 seconds following the offset of each movie during recall. We then computed a Pearson correlation coefficient across the mean within-movie event boundary pattern and the mean between-movie boundary pattern. A two-tailed one-sample *t*-test against zero was performed to test whether the group-level similarity between the two patterns was positive.

Testing the effect of audio amplitudes

Brief periods of silence were present at transitions between movies during both encoding and recall. During encoding, the 6-second title period between movies was silent. During recall, subjects often paused speaking for several seconds between recall of different movies. We tested whether the between-movie boundary patterns were associated with the absence of sound in general, as opposed to between-movie transitions specifically.

We first compared the activation pattern associated with any silent periods within movies during encoding and the activation pattern evoked by between-movie boundaries during recall (Figure 4, 'No sound' condition). To identify all periods of silence within the movies, we extracted the audio amplitudes of the movie clips (Figure 4 supplement 1A) by applying a Hilbert transform to the single-channel audio signals (44.1 kHz). The audio amplitudes were downsampled to match the temporal resolution of fMRI data (TR = 1.5 s), convolved with a double-gamma hemodynamic response function, and *z*-scored across time points. The periods of silence were defined as the within-movie time points (again excluding the first 45 seconds of each movie) whose audio amplitudes were equal to or lower than the mean amplitude of the time points corresponding to the silent between-movie title periods. For each subject and ROI, we averaged the activation patterns across these within-movie silent time periods to produce the mean activation pattern associated with the absence of sound. The mean pattern was then correlated with the between-movie boundary pattern produced by averaging 4.5 – 19.5 seconds following the offset of each movie during recall. A two-tailed one-sample *t*-test was performed to compare the group-level correlation coefficients against zero.

We additionally tested whether the time course of audio amplitude was correlated with the time course of pattern similarity (Pearson correlation) between the recall phase between-

movie boundary pattern and each time point of the encoding phase data (Figure 4 supplements 1B, 1C, 2). The time courses were generated for all time points within each movie, excluding the first 45 seconds of each movie. We first computed each subject's Pearson correlation coefficient between the two types of time courses. We then performed a group-level one-sample *t*-test against zero (two-tailed).

Acknowledgements

We thank Sarah DuBrow, Christopher J. Honey, and Megan T. deBettencourt for scientific discussions and comments on earlier versions of the manuscript. This work was supported by the Sloan Research Fellowship (J. C.) and Google Faculty Research Award (J. C.).

Competing interests

The authors declare no competing interests.

Citation diversity statement

Recent work in several fields of science has identified a bias in citation practices such that papers from women and other minority scholars are under-cited relative to the number of such papers in the field (Caplar et al., 2017; Dion et al., 2018; Dworkin et al., 2020; Maliniak et al., 2013; Mitchell et al., 2013). Here we sought to proactively consider choosing references that reflect the diversity of the field in thought, form of contribution, gender, race, ethnicity, and other factors. First, we obtained the predicted gender of the first and last author of each reference by using databases that store the probability of a first name being carried by a woman (Dworkin et al., 2020; Zhou et al., 2020). By this measure (and excluding self-citations to the first and last authors of our current paper), our references contain 13.64% woman(first)/woman(last), 15.91% man/woman, 25.87% woman/man, and 44.59% man/man. This method is limited in that a) names, pronouns, and social media profiles used to construct the databases may not, in every case, be indicative of gender identity and b) it cannot account for intersex, non-binary, or transgender people. Second, we obtained predicted racial/ethnic category of the first and last author of each reference by databases that store the probability of a first and last name being carried by an author of color (Ambekar et al., 2009; Sood & Laohaprapanon, 2018). By this measure (and excluding self-citations), our references contain 3.86% author of color (first)/author of color(last), 15.58% white author/author of color, 23.87% author of color/white author, and 56.69% white author/white author. This method is limited in that a) names, Census entries, and Wikipedia profiles used to make the predictions may not be indicative of racial/ethnic identity, and b) it cannot account for Indigenous and mixed-race authors, or those who may face differential biases due to the ambiguous racialization or ethnicization of their names. We look forward to future work that could help us to better understand how to support equitable practices in science.

References

Ambekar, A., Ward, C., Mohammed, J., Male, S., & Skiena, S. (2009). Name-ethnicity classification from open sources. *Proceedings of the 15th ACM SIGKDD International Conference on Knowledge Discovery and Data Mining*, 49–58. https://doi.org/10.1145/1557019.1557032

Baldassano, C., Chen, J., Zadbood, A., Pillow, J. W., Hasson, U., & Norman, K. A. (2017). Discovering event structure in continuous narrative perception and memory. *Neuron*, *95*(3), 709-721.e5. https://doi.org/10.1016/j.neuron.2017.06.041

Ben-Yakov, A., & Dudai, Y. (2011). Constructing realistic engrams: Poststimulus activity of hippocampus and dorsal striatum predicts subsequent episodic memory. *Journal of Neuroscience*, *31*(24), 9032–9042. https://doi.org/10.1523/JNEUROSCI.0702-11.2011

Ben-Yakov, A., Eshel, N., & Dudai, Y. (2013). Hippocampal immediate poststimulus activity in the encoding of consecutive naturalistic episodes. *Journal of Experimental Psychology: General*, *142*(4), 1255–1263. https://doi.org/10.1037/a0033558

Ben-Yakov, A., & Henson, R. N. (2018). The hippocampal film editor: Sensitivity and specificity to event boundaries in continuous experience. *Journal of Neuroscience*, *38*(47), 10057–10068. https://doi.org/10.1523/JNEUROSCI.0524-18.2018

Braga, R. M., & Buckner, R. L. (2017). Parallel interdigitated distributed networks within the individual estimated by intrinsic functional connectivity. *Neuron*, *95*(2), 457-471.e5. https://doi.org/10.1016/j.neuron.2017.06.038

Brunec, I. K., Moscovitch, M., & Barense, M. D. (2018). Boundaries shape cognitive representations of spaces and events. *Trends in Cognitive Sciences*, *22*(7), 637–650. https://doi.org/10.1016/j.tics.2018.03.013

Buckner, R. L., & DiNicola, L. M. (2019). The brain's default network: Updated anatomy, physiology and evolving insights. *Nature Reviews Neuroscience*, *20*(10), 593–608. https://doi.org/10.1038/s41583-019-0212-7

Bulkin, D. A., Sinclair, D. G., Law, L. M., & Smith, D. M. (2020). Hippocampal state transitions at the boundaries between trial epochs. *Hippocampus*, *30*(6), 582–595. https://doi.org/10.1002/hipo.23180

Caplar, N., Tacchella, S., & Birrer, S. (2017). Quantitative evaluation of gender bias in astronomical publications from citation counts. *Nature Astronomy*, *1*(6), 1–5. https://doi.org/10.1038/s41550-017-0141

Chen, J., Leong, Y. C., Honey, C. J., Yong, C. H., Norman, K. A., & Hasson, U. (2017). Shared memories reveal shared structure in neural activity across individuals. *Nature Neuroscience*, *20*(1), 115–125. https://doi.org/10.1038/nn.4450

Christoff, K., Irving, Z. C., Fox, K. C. R., Spreng, R. N., & Andrews-Hanna, J. R. (2016). Mind-wandering as spontaneous thought: A dynamic framework. *Nature Reviews Neuroscience*, *17*(11), 718–731. https://doi.org/10.1038/nrn.2016.113

Clewett, D., DuBrow, S., & Davachi, L. (2019). Transcending time in the brain: How event memories are constructed from experience. *Hippocampus*, *29*(3), 162–183. https://doi.org/10.1002/hipo.23074

Crittenden, B. M., Mitchell, D. J., & Duncan, J. (2015). Recruitment of the default mode network during a demanding act of executive control. *ELife*, *4*, e06481. https://doi.org/10.7554/eLife.06481

deBettencourt, M. T., Norman, K. A., & Turk-Browne, N. B. (2018). Forgetting from lapses of sustained attention. *Psychonomic Bulletin & Review*, *25*(2), 605–611. https://doi.org/10.3758/s13423-017-1309-5

Dion, M. L., Sumner, J. L., & Mitchell, S. M. (2018). Gendered citation patterns across political science and social science methodology fields. *Political Analysis*, *26*(3), 312–327. https://doi.org/10.1017/pan.2018.12

DuBrow, S., Rouhani, N., Niv, Y., & Norman, K. A. (2017). Does mental context drift or shift? *Current Opinion in Behavioral Sciences*, *17*, 141–146. https://doi.org/10.1016/j.cobeha.2017.08.003

Dworkin, J. D., Linn, K. A., Teich, E. G., Zurn, P., Shinohara, R. T., & Bassett, D. S. (2020). The extent and drivers of gender imbalance in neuroscience reference lists. *Nature Neuroscience*, *23*(8), 918–926. https://doi.org/10.1038/s41593-020-0658-y

Fox, M. D., Snyder, A. Z., Barch, D. M., Gusnard, D. A., & Raichle, M. E. (2005). Transient BOLD responses at block transitions. *NeuroImage*, *28*(4), 956–966. https://doi.org/10.1016/j.neuroimage.2005.06.025

Hasselmo, M. E. (1995). Neuromodulation and cortical function: modeling the physiological basis of behavior. *Behavioural Brain Research*, *67*(1), 1–27. https://doi.org/10.1016/0166-4328(94)00113-T

Hasson, U., Chen, J., & Honey, C. J. (2015). Hierarchical process memory: memory as an integral component of information processing. *Trends in Cognitive Sciences*, *19*(6), 304–313.

Honey, C. J., Newman, E. L., & Schapiro, A. C. (2017). Switching between internal and external modes: A multiscale learning principle. *Network Neuroscience*, *1*(4), 339–356. https://doi.org/10.1162/NETN_a_00024

Karapanagiotidis, T., Vidaurre, D., Quinn, A. J., Vatansever, D., Poerio, G. L., Turnbull, A., Ho, N. S. P., Leech, R., Bernhardt, B. C., Jefferies, E., Margulies, D. S., Nichols, T. E., Woolrich, M. W., & Smallwood, J. (2020). The psychological correlates of distinct neural states occurring during wakeful rest. *Scientific Reports*, *10*(1), 21121. https://doi.org/10.1038/s41598-020-77336-z

Kragel, J. E., & Polyn, S. M. (2015). Functional interactions between large-scale networks during memory search. *Cerebral Cortex*, *25*(3), 667–679. https://doi.org/10.1093/cercor/bht258

Lee, H., & Chen, J. (2021). Narratives as networks: Predicting memory from the structure of naturalistic events. *BioRxiv*, 2021.04.24.441287. https://doi.org/10.1101/2021.04.24.441287

Maliniak, D., Powers, R., & Walter, B. F. (2013). The gender citation gap in international relations. *International Organization*, *67*(4), 889–922. https://doi.org/10.1017/S0020818313000209

Manning, J. R., Hulbert, J. C., Williams, J., Piloto, L., Sahakyan, L., & Norman, K. A. (2016). A neural signature of contextually mediated intentional forgetting. *Psychonomic Bulletin & Review*, *23*(5), 1534–1542. https://doi.org/10.3758/s13423-016-1024-7

Medvedeva, A., Saw, R., Silvestri, C., Sirota, M., Fuggetta, G., & Galli, G. (2021). Offset-related brain activity in the left ventrolateral prefrontal cortex promotes long-term memory formation of verbal events. *Brain Stimulation*, *14*(3), 564–570. https://doi.org/10.1016/j.brs.2021.03.002

Mildner, J. N., & Tamir, D. I. (2019). Spontaneous thought as an unconstrained memory process. *Trends in Neurosciences*, *42*(11), 763–777. https://doi.org/10.1016/j.tins.2019.09.001

Mitchell, S. M., Lange, S., & Brus, H. (2013). Gendered citation patterns in international relations journals. *International Studies Perspectives*, *14*(4), 485–492. https://doi.org/10.1111/insp.12026

Mittner, M., Hawkins, G. E., Boekel, W., & Forstmann, B. U. (2016). A neural model of mind wandering. *Trends in Cognitive Sciences*, *20*(8), 570–578. https://doi.org/10.1016/j.tics.2016.06.004

Mortaheb, S., Klados, M. A., Calster, L. V., Boulakis, P. A., Georgoula, K., Majerus, S., & Demertzi, A. (2021). Mind blanking is associated with a rigid spatio-temporal profile in typical wakefulness. *BioRxiv*, 2021.05.10.443428. https://doi.org/10.1101/2021.05.10.443428

Ranganath, C., & Ritchey, M. (2012). Two cortical systems for memory-guided behaviour. *Nature Reviews Neuroscience*, *13*(10), 713–726. https://doi.org/10.1038/nrn3338

Reagh, Z. M., Delarazan, A. I., Garber, A., & Ranganath, C. (2020). Aging alters neural activity at event boundaries in the hippocampus and Posterior Medial network. *Nature Communications*, *11*(1), 3980. https://doi.org/10.1038/s41467-020-17713-4

Ritchey, M., & Cooper, R. A. (2020). Deconstructing the posterior medial episodic network. *Trends in Cognitive Sciences*, *24*(6), 451–465. https://doi.org/10.1016/j.tics.2020.03.006

Schaefer, A., Kong, R., Gordon, E. M., Laumann, T. O., Zuo, X.-N., Holmes, A. J., Eickhoff, S. B., & Yeo, B. T. T. (2018). Local-global parcellation of the human cerebral cortex from intrinsic functional connectivity MRI. *Cerebral Cortex*, *28*(9), 3095–3114. https://doi.org/10.1093/cercor/bhx179

Schapiro, A. C., Rogers, T. T., Cordova, N. I., Turk-Browne, N. B., & Botvinick, M. M. (2013). Neural representations of events arise from temporal community structure. *Nature Neuroscience*, *16*(4), 486–492. https://doi.org/10.1038/nn.3331

Shin, Y. S., & DuBrow, S. (2021). Structuring memory through inference-based event segmentation. *Topics in Cognitive Science*, *13*(1), 106–127. https://doi.org/10.1111/tops.12505

Smallwood, J., & Schooler, J. W. (2015). The science of mind wandering: Empirically navigating the stream of consciousness. *Annual Review of Psychology*, *66*(1), 487–518. https://doi.org/10.1146/annurev-psych-010814-015331

Smith, V., Mitchell, D. J., & Duncan, J. (2018). Role of the default mode network in cognitive transitions. *Cerebral Cortex*, *28*(10), 3685–3696. https://doi.org/10.1093/cercor/bhy167

Song, H., Finn, E. S., & Rosenberg, M. D. (2021). Neural signatures of attentional engagement during narratives and its consequences for event memory. *Proceedings of the National Academy of Sciences*, *118*(33). https://doi.org/10.1073/pnas.2021905118

Sood, G., & Laohaprapanon, S. (2018). Predicting race and ethnicity from the sequence of characters in a name. *ArXiv:1805.02109 [Stat]*. http://arxiv.org/abs/1805.02109

Speer, N. K., Zacks, J. M., & Reynolds, J. R. (2007). Human brain activity time-locked to narrative event boundaries. *Psychological Science*, *18*(5), 449–455. https://doi.org/10.1111/j.1467-9280.2007.01920.x

Sripada, C., & Taxali, A. (2020). Structure in the stream of consciousness: Evidence from a verbalized thought protocol and automated text analytic methods. *Consciousness and Cognition*, *85*, 103007. https://doi.org/10.1016/j.concog.2020.103007

Tseng, J., & Poppenk, J. (2020). Brain meta-state transitions demarcate thoughts across task contexts exposing the mental noise of trait neuroticism. *Nature Communications*, *11*(1), 3480. https://doi.org/10.1038/s41467-020-17255-9

Ward, A. F., & Wegner, D. M. (2013). Mind-blanking: when the mind goes away. *Frontiers in Psychology*, *0*. https://doi.org/10.3389/fpsyg.2013.00650

Wen, T., Duncan, J., & Mitchell, D. J. (2020). Hierarchical representation of multistep tasks in multiple-demand and default mode networks. *Journal of Neuroscience*, *40*(40), 7724–7738. https://doi.org/10.1523/JNEUROSCI.0594-20.2020

Zacks, J. M. (2020). Event perception and memory. *Annual Review of Psychology*, *71*(1), 165–191. https://doi.org/10.1146/annurev-psych-010419-051101

Zacks, J. M., Braver, T. S., Sheridan, M. A., Donaldson, D. I., Snyder, A. Z., Ollinger, J. M., Buckner, R. L., & Raichle, M. E. (2001). Human brain activity time-locked to perceptual event boundaries. *Nature Neuroscience*, *4*(6), 651–655. https://doi.org/10.1038/88486

Zacks, J. M., Kurby, C. A., Eisenberg, M. L., & Haroutunian, N. (2011). Prediction error associated with the perceptual segmentation of naturalistic events. *Journal of Cognitive Neuroscience*, *23*(12), 4057–4066. https://doi.org/10.1162/jocn_a_00078

Zacks, J. M., Speer, N. K., Swallow, K. M., Braver, T. S., & Reynolds, J. R. (2007). Event perception: A mind-brain perspective. *Psychological Bulletin*, *133*(2), 273–293. https://doi.org/10.1037/0033-2909.133.2.273

Zacks, J. M., Speer, N. K., Swallow, K. M., & Maley, C. J. (2010). The brain's cutting-room floor: Segmentation of narrative cinema. *Frontiers in Human Neuroscience*, *0*. https://doi.org/10.3389/fnhum.2010.00168

Zheng, J., Schjetnan, A. G. P., Yebra, M., Mosher, C., Kalia, S., Valiante, T. A., Mamelak, A. N., Kreiman, G., & Rutishauser, U. (2021). Cognitive boundary signals in the human medial temporal lobe shape episodic memory representation. *BioRxiv*, 2021.01.16.426538. https://doi.org/10.1101/2021.01.16.426538

Zhou, D., Cornblath, E. J., Stiso, J., Teich, E. G., Dworkin, J. D., Blevins, A. S., & Bassett, D. S. (2020). *Gender diversity statement and code notebook v1.0*. Zenodo. https://doi.org/10.5281/zenodo.3672110

Supplementary information

Figure 1 supplement 1 (video). Changes in univariate activation at between-movie boundaries during recall. The animation shows the time series of whole-brain activation maps (BOLD signals z-scored across all volumes within a scanning run) locked to the offset of the recall of each movie, from 30 seconds before to 45 seconds after the offset. Within each of the 7.5-second time windows shown as a red bar on the time axis, BOLD signals in each vertex were averaged across time points, movies, and subjects. Blue-cyan areas indicate regions with lower-than-average activation. Red-yellow areas indicate regions with higher-than-average activation.

Figure 1 supplement 2 (video). Changes in univariate activation at between-movie boundaries during encoding. The animation shows the time series of whole-brain activation maps (BOLD signals z-scored across all volumes within a scanning run) locked to the offset of each movie clip during the encoding phase, from 30 seconds before to 45 seconds after the offset. Within each of the 7.5-second time windows shown as a red bar on the time axis, BOLD signals in each vertex were averaged across time points, movies, and subjects. Blue-cyan areas indicate regions with lower-than-average activation. Red-yellow areas indicate regions with higher-than-average activation.

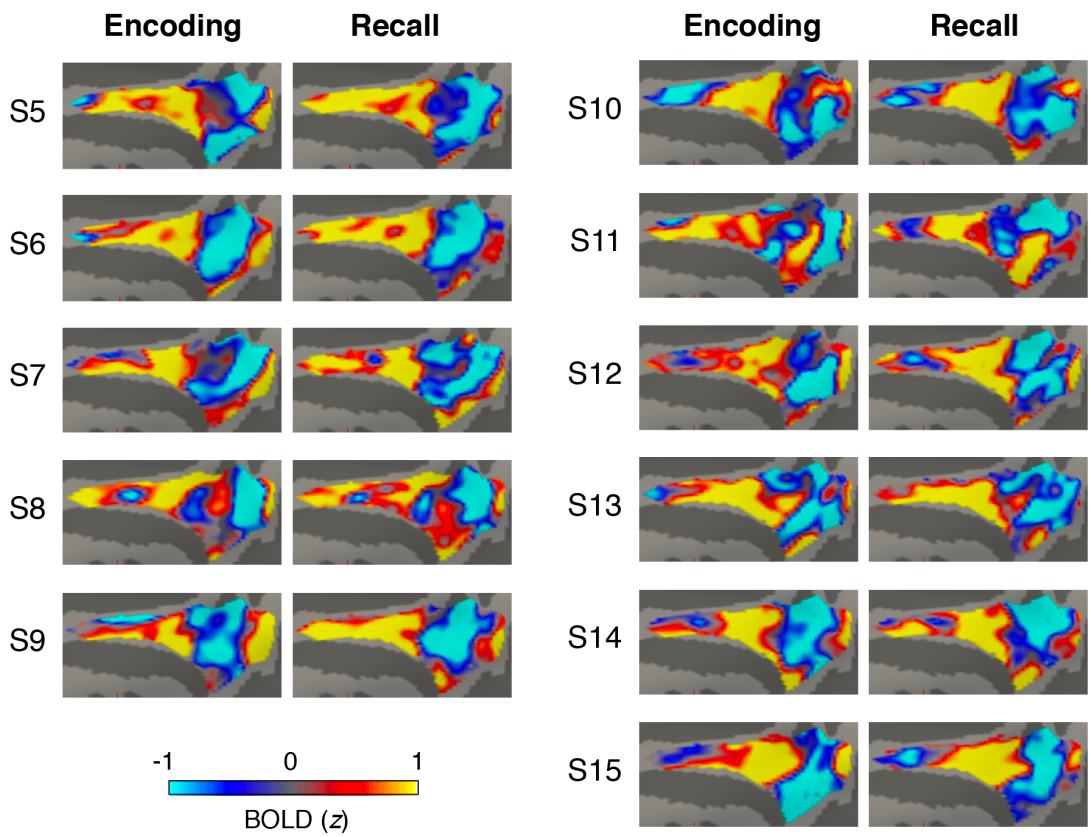

Figure 3 supplement 1. Subject-specific boundary patterns in the posterior medial cortex (PMC). The between-movie boundary patterns were averaged across all movies and then *z*-scored across vertices within the PMC ROI mask, separately for the encoding phase and the recall phase. PMC of 11 subjects (S5 – 15) are shown on the medial surface of the right hemisphere of the fsaverage6 template brain.

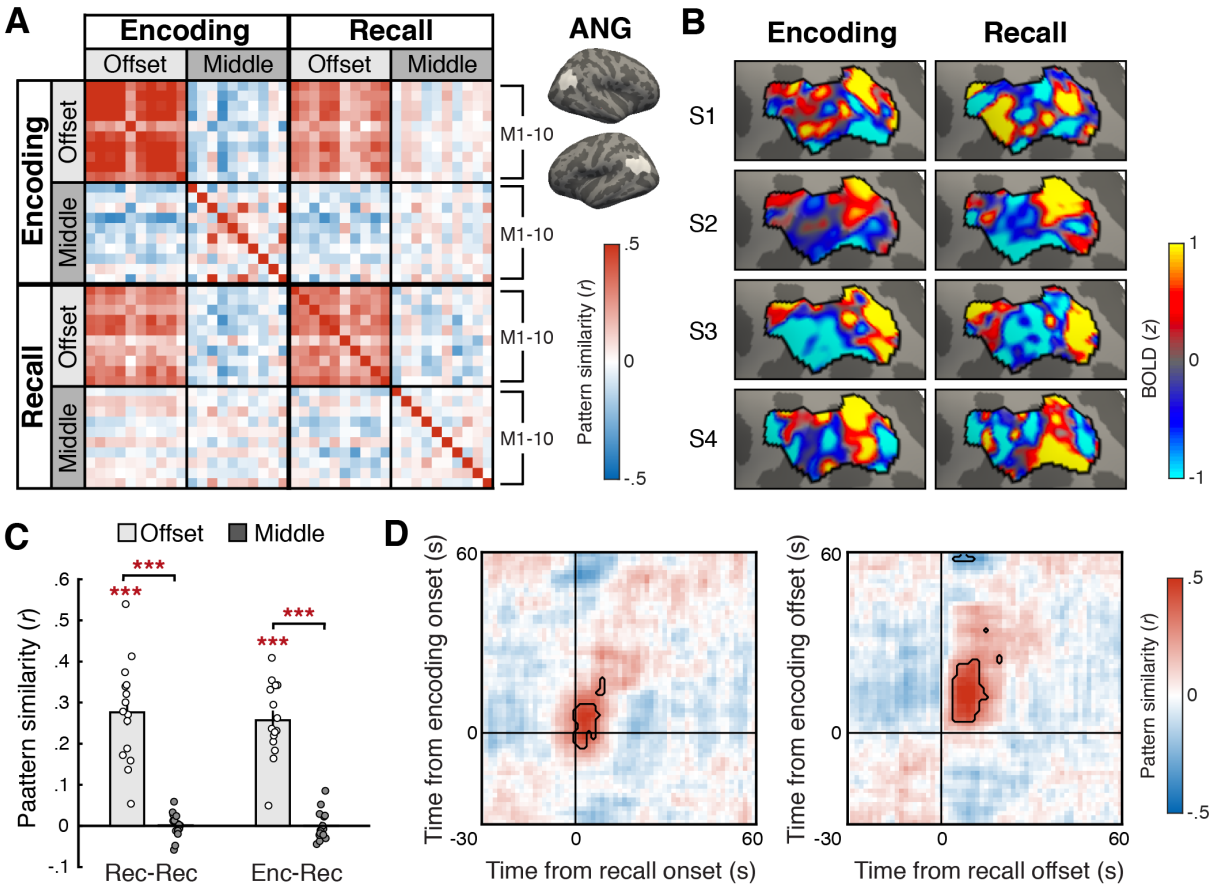

Figure 3 supplement 2. Boundary pattern in the angular gyrus (ANG). (A) ANG activation pattern similarity (Pearson correlation) between the 10 movie stimuli (M1 – 10), conditions (Offset = Boundary, Middle = Non-boundary), and experimental phases (Encoding, Recall), averaged across all subjects. The boundary pattern of a movie was defined as the mean pattern averaged across the 15-second window following the offset of the movie. The non-boundary pattern was defined as the mean pattern averaged across the 15-second window in the middle of a movie. The time windows for both boundary and non-boundary patterns were shifted forward by 4.5 seconds to account for the hemodynamic response delay. ANG regions of interest are shown as white areas on the inflated surface of a template brain. (B) Subject-specific mean activation patterns associated with between-movie boundaries during encoding (left) and recall (right). The boundary patterns were averaged across all movies and then *z*-scored across vertices within the ANG ROI mask, separately for each experimental phase. ANG (demarcated by black outlines) of four example subjects (S1 – 4) are shown on the lateral surface of the left hemisphere of the fsaverage6 template brain. (C) Within-phase (Recall-Recall) and between-phase (Encoding-Recall) pattern similarity across different movies, computed separately for the boundary (Offset)

and non-boundary (Middle) patterns in ANG. Bar graphs show the mean across subjects. Circles represent individual subjects. Error bars show SEM across subjects. ***$p < .001$. (D) Time-point-by-time-point ANG pattern similarity across the encoding phase and recall phase activation patterns around between-movie boundaries, averaged across all subjects. The time series of activation patterns were locked to either the onset (left) or the offset (right) of each movie. Note that in this figure, zero corresponds to the true stimulus/behavior time, with no shifting for hemodynamic response delay. Areas outlined by black lines indicate correlations significantly different from zero after multiple comparisons correction (Bonferroni corrected $p < .05$).

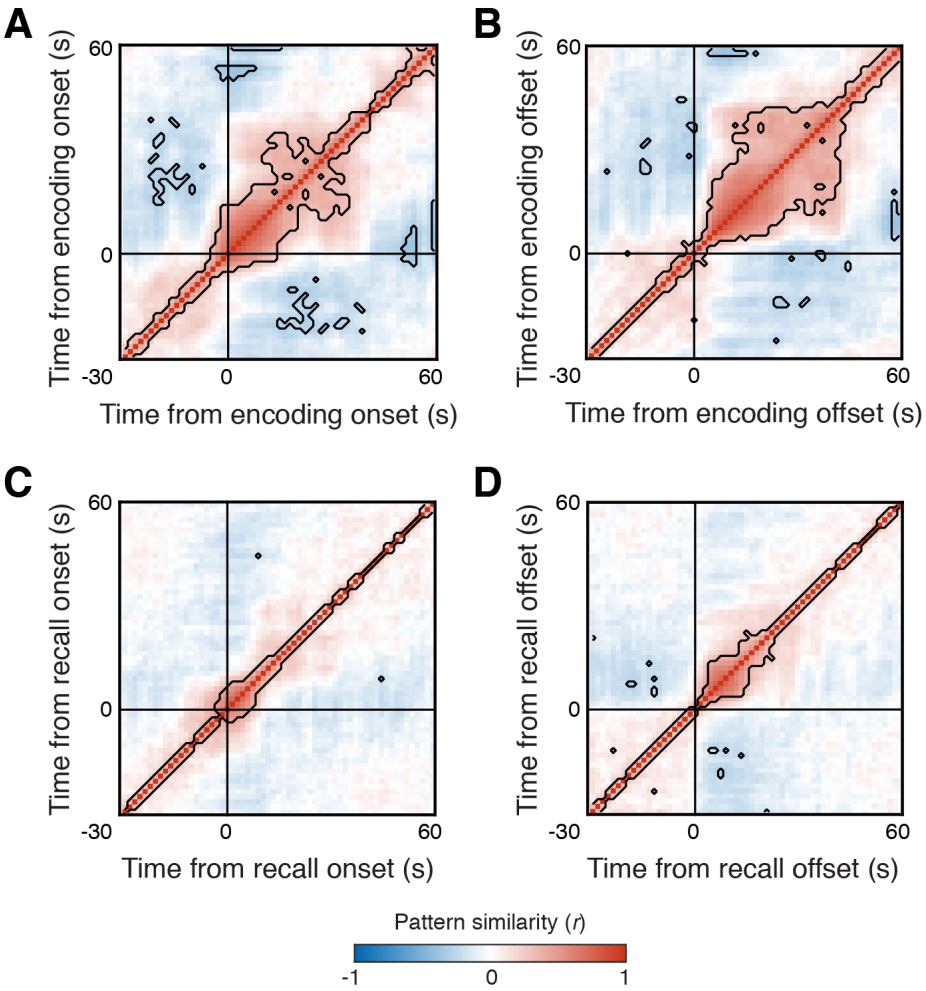

Figure 3 supplement 3. Time-time pattern similarity in the posterior medial cortex (PMC). The similarity matrices show Pearson correlations between PMC patterns across time points around between-movie boundaries during encoding (A & B) and recall (C & D), calculated within each subject and then averaged across all subjects. The time series of activation patterns were locked to either the onset (A & C) or the offset (B & D) of each movie. Boundary patterns were likely to be evoked by the offset rather than the onset of movies. Note that in this figure, zero corresponds to the true stimulus/behavior time, with no shifting for hemodynamic response delay. Areas outlined by black lines indicate correlations significantly deviate from zero after multiple comparisons correction (Bonferroni corrected $p < .05$).

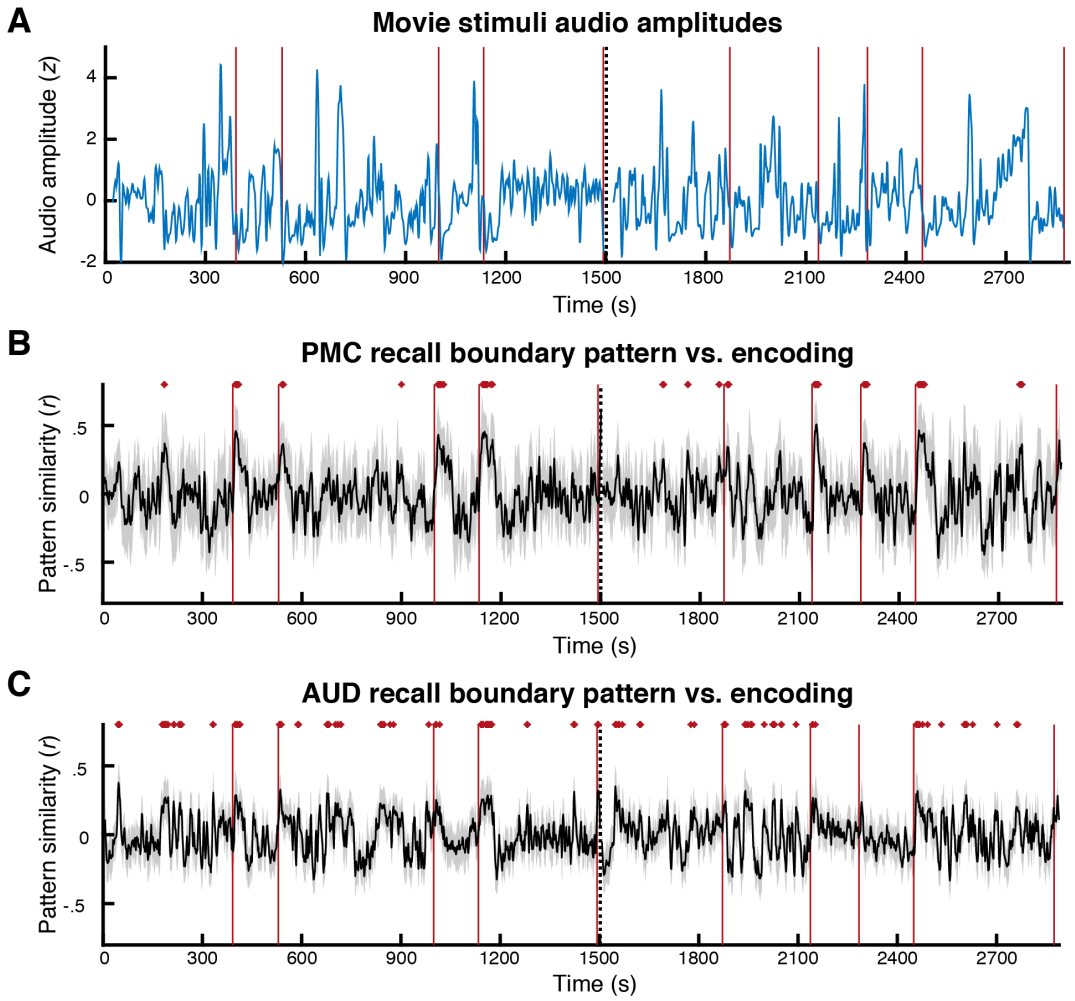

Figure 4 supplement 1. Time series of audio amplitudes during encoding and the similarity to the recall boundary pattern. (A) Audio amplitudes of the movie stimuli. The audio amplitudes were convolved with a hemodynamic response function and *z*-scored across time points. (B) Posterior medial cortex (PMC) pattern similarity (Pearson correlation) between each volume of encoding data and the template between-movie boundary pattern measured during recall (average of 4.5 – 19.5 seconds from the offset of each recalled movie). (C) Auditory cortex (AUD) pattern similarity between each volume of encoding data and the template between-movie boundary pattern measured during recall. In A, B, and C, the vertical dotted line in the middle indicates the boundary between the two encoding scanning runs. Vertical red lines indicate the offsets of each movie clip. In B and C, black lines show the mean across subjects. Shaded areas indicate the standard deviation across subjects. Red dots mark time points that showed significantly positive pattern correlations after multiple comparisons correction across time points (Bonferroni corrected $p < .05$).

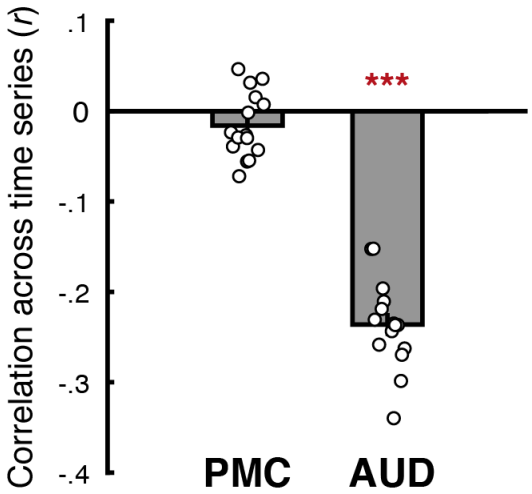

Figure 4 supplement 2. Relationship between audio amplitudes during encoding and the similarity to the recall boundary pattern. We computed correlations between the time series of audio amplitudes and the time series of similarity between the boundary pattern and each volume of encoding data in the posterior medial cortex (PMC) and the auditory cortex (AUD). Time points within each of the ten movies after excluding the first 45 seconds were included in the analysis. PMC correlations were not significantly different from zero ($t(14) = 1.7$, $p = .11$, Cohen's $d_z = .44$), whereas AUD showed significantly negative correlations ($t(14) = 18.66$, $p < .001$, Cohen's $d_z = 4.82$). Bar graphs show the mean across subjects. Circles represent individual subjects. Error bars show SEM across subjects. ***$p < .001$ against zero.